PCCP

PAPER

Cite this: *Phys. Chem. Chem. Phys.*, 2014, **16**, 23340

$M(BH_3NH_2BH_2NH_2BH_3)$ – the missing link in the mechanism of the thermal decomposition of light alkali metal amidoboranes†

K. J. Fijalkowski,*[a] T. Jaroń,[a] P. J. Leszczyński,[a] E. Magos-Palasyuk,[b] T. Palasyuk,[b] M. K. Cyrański[c] and W. Grochala*[a]

Received 24th July 2014,
Accepted 8th September 2014

DOI: 10.1039/c4cp03296a

www.rsc.org/pccp

We report a novel family of hydrogen-rich materials – alkali metal di(amidoborane)borohydrides, $M(BH_3NH_2BH_2NH_2BH_3)$. The title compounds are related to metal amidoboranes (amidotrihydroborates) but have higher gravimetric H content. Li salt contains 15.1 wt% H and discharges very pure H_2 gas. Differences in thermal stability between amidoboranes and respective oligoamidoboranes explain the release of the ammonia impurity (along with H_2) during the thermal decomposition of light alkali amidoboranes, $LiNH_2BH_3$, $NaNH_2BH_3$ and $NaLi(NH_2BH_3)_2$, and confirm the mechanism of the side decomposition reaction.

Introduction

Protonic-hydridic materials (XH_xYH_y) comprise an important family of highly efficient hydrogen stores in the solid state.[1,2] The simultaneous presence of acidic H^+ (attached to a more electronegative element, X) and basic H^- (attached to a more electropositive element, Y) results in low energy barrier and, concomitantly, in low temperature H_2 desorption from these materials. Systems based on X = nitrogen and Y = boron constitute the most researched protonic-hydridic hydrogen stores.[3,4] These encompass amide-borohydrides,[5,6] NH_4BH_4,[7] ammonia borane (NH_3BH_3),[8,9] as well as its derivatives, such as metal amidoboranes, MNH_2BH_3 (MAB phases).[10–21] Most of these materials suffer from unfavorable thermodynamics, which precludes the re-absorption of H_2 by the discharged residue of the thermal decomposition. Despite emitting impure H_2 gas, the large gravimetric H content (up to 24.4 wt% for NH_4BH_4) renders them attractive to be H storage media for mobile technologies due to their off-board regeneration.

Here, we describe a novel family of hydrogen rich materials – metal di(amidoborane)borohydrides, $M(BH_3NH_2BH_2NH_2BH_3)$ (M(B3N2) phases), as exemplified by lithium and sodium derivatives. The M(B3N2) phases may formally be regarded to be the derivatives of metal borohydrides, $M[B(H)_2(NH_2BH_3)_2]$ (analogous to the known $M[B(H)_x(CN)_{4-x}]$, $M[B(H)_x(CH_3)_{4-x}]$ or $M[B(H)_x(C_2H_5)_{4-x}]$ salts). The M(B3N2) compounds have much larger gravimetric hydrogen capacity than MAB phases and they fulfill the DOE gravimetric target in excess [Li(B3N2), 15.1 wt% H; Na(B3N2), 12.6 wt% H], which is crucial when designing the storage system (consisting of both: storage material and various mechanical elements) to contain more than 7.5 wt% of hydrogen (Fig. 1).

Here, we show that the M(B3N2) derivatives constitute the missing link in the mechanism of the thermal decomposition of light alkali metal amidoboranes [LiAB, NaAB and $NaLi(AB)_2$]. The transformation of MABs to the corresponding ammonia containing $[M(NH_3)](B3N2)$ and then the formation of M(B3N2) is responsible for the presence of ammonia impurity in the H_2 gas evolved from MABs.[17,22,23] Moreover, the M(B3N2) salts thermally decompose above 140–160 °C and release more than 50% of their total H content up to 200 °C. Importantly, Li salt yields H_2 gas that is virtually free from any impurities.

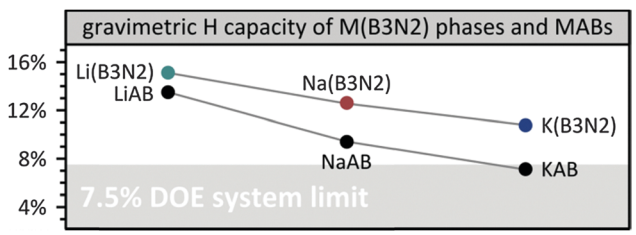

Fig. 1 Comparison of total theoretical hydrogen capacity of light alkali metal M(B3N2) phases and respective amidoboranes, M = Li, Na, K without taking into account weight of other elements of the storage system.

[a] *Center of New Technologies, University of Warsaw, ul. Zwirki i Wigury 93, 02-089 Warsaw, Poland. E-mail: w.grochala@cent.uw.edu.pl, karol.fijalkowski@cent.uw.edu.pl*
[b] *Institute of Physical Chemistry, Polish Academy of Sciences, ul. Kasprzaka 44/52, 01-224 Warsaw, Poland*
[c] *Faculty of Chemistry, University of Warsaw, ul. Pasteura 1, 02-093 Warsaw, Poland*

† Electronic supplementary information (ESI) available. See DOI: 10.1039/c4cp03296a

Results and discussion

The first MB_xN_y salt with $x > y$ was probably synthesized three quarters of a century ago, when Schlesinger and Burg in 1938 reported a light porous solid of a general formula NaB_2H_8N, obtained in the reaction of diammoniate of diborane with metallic sodium.[24] The product has been incompletely characterized and these results have not been repeated by others. In 2009, we observed evolution of ammonia-along with H_2-during the thermal decomposition of alkali metal amidoboranes.[22] Elimination of a volatile nitrogen compound suggested the formation of a solid residue, which was richer in boron as compared to the parent 1 : 1 stoichiometry of metal amidoboranes. At that time, the formation of the "NB_2" metal derivatives in the solid state was suggested,[22,23] which is in accordance with the claim from Schlesinger and Burg.[24]

Probably Li(B3N2) and Na(B3N2) compounds were first observed by Evans in 2011.[25] The work, however, missed the basic characterization data, such as correct stoichiometry and crystal structure, essential for the chemical identity of the compounds. Experimental data contained in investigations by Ryan, 2011,[26] did not present new structural evidence but suggested the formation of a new crystalline compound, which is built of lithium cations and five-membered anionic chains with the BNBNB skeleton. The presence of pentameric moieties has recently been suggested for the sodium compound by W. C. Ewing *et al.*,[27] 2013. The reported ^{11}B NMR spectrum revealed the presence of $(BH_2)_1(BH_3)_2$ constituents of the anions. The authors, however, did not present any data on the crystal structure of the studied material.

We have now conducted a systematic study of the two lightest alkali metal M(B3N2) phases (M = Li or Na) using ^{11}B NMR, single crystal and powder X-ray diffraction, IR absorption, Raman scattering, thermogravimetry and differential scanning calorimetry. We have been able to solve the crystal structures of the M(B3N2) phases (M = Li or Na) and provide complete physicochemical characterization in relation to the hydrogen storage properties. The comparative analysis of the M(B3N2) phases with their MABs analogues has been also carried out.

M(B3N2) phases were conveniently obtained in the reaction of ammonia borane with respective metal hydride in molar ratio 3 : 1 in anhydrous THF (see ESI†):

$$MH + 3NH_3BH_3 \rightarrow M(BH_3NH_2BH_2NH_2BH_3) + NH_3\uparrow + 2H_2\uparrow \quad (1)$$

Mechanochemical synthesis followed by thermal desorption of excess NH_3 is an alternative approach[25] (ESI†).

Alkali metal M(B3N2) phases are white low-density solids which are sensitive to moisture. Li(B3N2) and Na(B3N2) are stable at room temperature in contrast to respective MABs,[23] as discussed below. Li(B3N2) is well soluble in THF, in contrast to Na(B3N2). However, the solubility of both compounds is sufficient to obtain the ^{11}B NMR spectra (Fig. 2). The spectra are different from those of the respective metal amidoboranes (see ESI†) and they reveal the presence of a characteristic quarter at *ca.* −21 ppm representing $[BH_3]$ groups and a twice weaker triplet at *ca.* −8 ppm representing $[BH_2]$ moieties, thus confirming the presence of the $(BH_2)_1(BH_3)_2$ constituents of the anions. The spectra also confirm the presence of small amount of LiAB impurity in the sample of Li(B3N2).

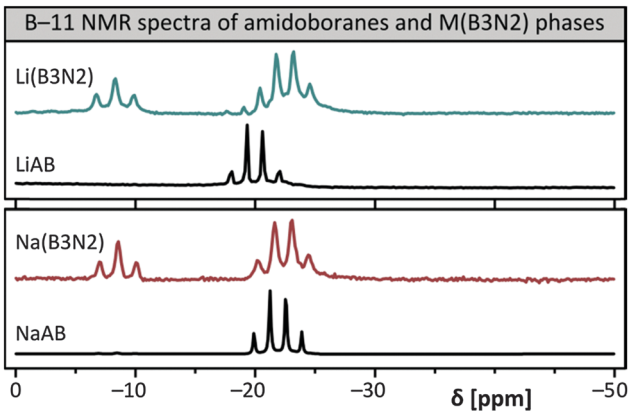

Fig. 2 Comparison of ^{11}B NMR spectra in THF-d_8 of M(B3N2) phases (coloured lines) and metal amidoboranes (black lines): lithium salts (top) and sodium salts (bottom).

All alkali metal M(B3N2) phases are characterized by similar and characteristic Raman (Fig. 3) and FTIR spectra (ESI†), which are easily distinguishable from the spectra of respective metal amidoboranes (MABs). In general, the sharp doublet in the Raman spectra assigned to the symmetric NH stretching modes appears at smaller wavenumbers for M(B3N2) phases than for the respective MABs. Simultaneously, the most intense BH stretching bands fall at higher wavenumbers for M(B3N2) phases than for the respective MABs. These features suggest that the N–H bonds are considerably weaker for M(B3N2) phases than for MABs, while the opposite holds true for the B–H bonds. Although the stiffening of the B–H modes is in qualitative agreement with the trend predicted from our DFT calculations for the isolated $(NH_2BH_3)^-$ and $(BH_3NH_2BH_2NH_2BH_3)^-$ anions in the gas phase, the softening of the N–H bonds observed in experiment is in disagreement with the computed trend (see ESI†), and it likely originates from the solid state effects (differences of packing,

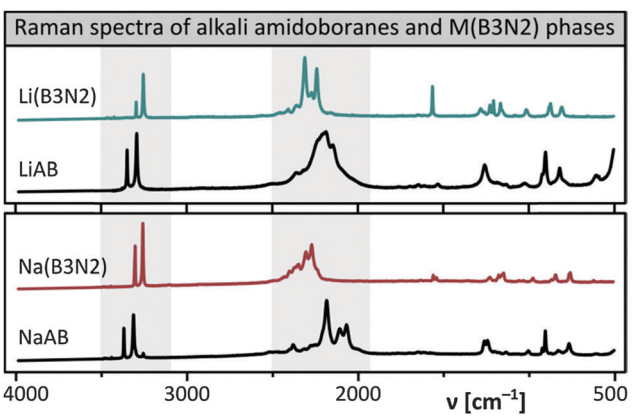

Fig. 3 Comparison of Raman spectra of M(B3N2) phases (coloured lines) and metal amidoboranes (black lines): lithium salts (top) and sodium salts (bottom). The NH (3200–3400 cm^{-1}) and BH (1900–2500 cm^{-1}) stretching regions are highlighted.

interactions of anions with cations, or secondary interactions, such as possible dihydrogen bonding).

One sharp band appearing for the HNH bending vibration at 1571 cm^{-1} is seen in the Raman spectrum of Li(B3N2); the presence of a single band suggests that the NH_2 groups have identical local symmetry (thus, only the in-phase HNH bending is Raman-active). Indeed, the $(BH_3NH_2BH_2NH_2BH_3)^-$ moiety in the crystal structure of Li(B3N2) is found in the *n*-alkane-like quasi-linear geometry with two crystallographically equivalent NH_2 units.

The samples of alkali metal M(B3N2) phases were studied with powder X-ray diffraction (PXD) (Fig. 4).

Lattice parameters of Li(B3N2) determined in this work are in accordance with the values obtained for the compounds reported by Evans[25] and by Ryan[26] (Table 1 and ESI†). This result suggests that chemical identity of all three crystalline samples may be the same, even though Evans suggested a different stoichiometry for this compound. Evans proposed the chemical formula of $Li(NH_3)^+(BH_3NH_2BH_3)^-$ containing the ammonia molecule weakly bound to alkali metal cation.[25] Results of our spectroscopic measurements (Raman or IR), however, did not reveal any significant bands in the 3350–3400 cm^{-1} region, which is characteristic for $Li(NH_3)^+$ cations. Moreover, we observed that Li(B3N2) releases pure hydrogen on heating, which corroborates the absence of the $Li(NH_3)^+$ cation in material. Based on the combination of NMR, FTIR, and Raman spectra, as well as PXD we have been able to confirm the stoichiometry of $Li(BH_3NH_2BH_2NH_2BH_3)$ which was previously suggested by Ryan.[26] The crystal structure of Li(B3N2) consists of Li^+ layers which are linked *via* five member chain $(BH_3NH_2BH_2NH_2BH_3)^-$ anions which coordinate lithium cations using the hydrogen atoms of terminal $[BH_3]$ groups only (Fig. 5). It should be recalled that the N atoms of the $(BH_3NH_2BH_2NH_2BH_3)^-$ anions do not have any lone pairs available for coordination to metal centers; thus, only the basic hydride anions at boron may be used for bonding. Lithium cations are found in tetrahedral coordination of four hydrogen atoms, resembling those found for the orthorhombic form of $LiBH_4$, and they are different from the first coordination sphere of Li in LiAB

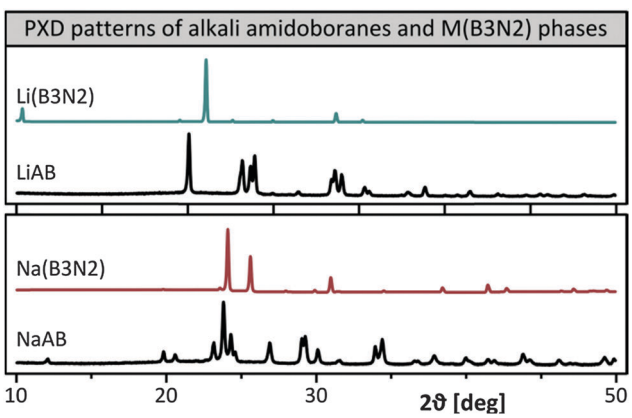

Fig. 4 Comparison of PXD patterns of M(B3N2) phases (coloured lines) and respective amidoboranes (black lines): lithium (top) and sodium salts (bottom).

Table 1 Comparison of lattice parameters for three alkali metal M(B3N2) phases

Compound	System	Space group	*a* [Å]	*c* [Å]	*V* [Å^3]	*Z*
Li(B3N2)[a]	Tetragonal	$P\bar{4}2c$	4.02 (1)	16.95 (5)	273.9 (12)	2
Na(B3N2)[b]	Hexagonal	$P6_3/m$	4.3392 (2)	17.853 (6)	291.11 (18)	2

[a] Compare ref. 25 and 26. [b] Compare ref. 25.

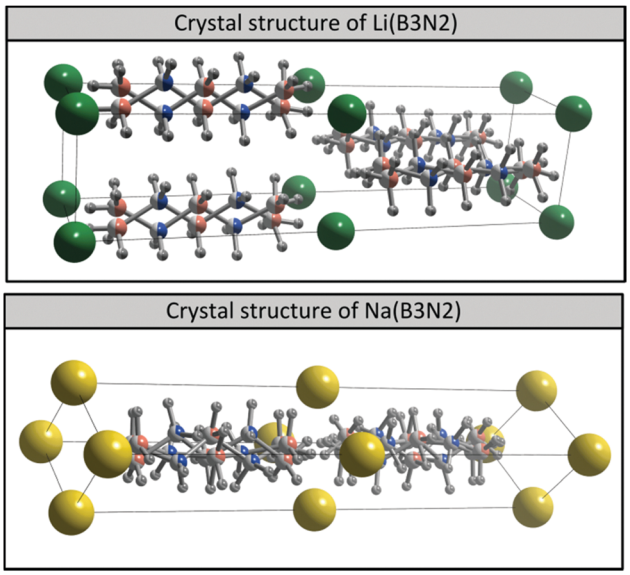

Fig. 5 Crystal structure of alkali metal M(B3N2) phases as determined by PXD: H – grey, B – red, N – blue, Li – green, Na – yellow. Li(B3N2) top and Na(B3N2) – bottom. Crystallographic positions with partial population are marked with partly-colored balls.

(the N_1H_4 coordination). The shortest Li–H distance is 2.0(2) Å (as compared with the corresponding distance of 1.98(1) Å in *Pbca* LiAB[28] and 1.98(1) Å in *Pnma* $LiBH_4$[29]). The average B–N bond length of the $(BH_3NH_2BH_2NH_2BH_3)^-$ anion is *ca.* 1.59(6) Å (as compared with 1.55 Å for LiAB[10]), whereas the average angles between the B–N bonds (115°) are close to the tetrahedral angle. The crystal structure contains disordered $(BH_3NH_2BH_2NH_2BH_3)^-$ anions lying along the *z* axis of the unit cell. Importantly, the inter-anion dihydrogen bonds are absent in the crystal structure of Li(B3N2).

The volume of Li(B3N2) per one formula unit, 136.95(6) Å^3, is smaller by only 3.3% than the expected volume of this compound (141.65 Å^3), which may be derived from the following equation:

$$V[Li(BH_3NH_2BH_2NH_2BH_3)] = 3V[Li(NH_2BH_3)] - V[LiNH_2] - V[LiH] \quad (2)$$

The PXD for Na(B3N2) yields a diffraction pattern which can be indexed using the trigonal cell proposed by Evans.[25] We have determined the crystal structure of Na(B3N2) in a centrosymmetric primitive hexagonal $P6_3/m$ cell with $Z = 2$ (Table 1 and ESI†). There are three important similarities between crystal structures of Na(B3N2) and Li(B3N2): first, Na(B3N2) also consists of metal

cation layers separated by layers containing the $(BH_3NH_2BH_2NH_2BH_3)^-$ anions. Second, the anions are substantially disordered along the z axis. Third, metal cations are found in the homoleptic environment of hydrogen atoms of the terminal $[BH_3]$ groups. As a consequence, sodium cations exhibit a coordination with 8 H atoms ($=12 \times \frac{2}{3}$), and the closest Na–H distance is 2.22(9) Å. This may be compared to the shortest Na–H separation of *ca.* 2.33 Å, which is seen for NaAB (*cf.* ESI†) and a much larger value of *ca.* 2.58 Å, which is typical of the disordered room-temperature rocksalt form of $NaBH_4$.[30] Obviously, the metal–hydrogen bond lengths that are listed here for both M(B3N2) salts are not exact because of the inherent problems related with solving disordered crystal structures of compounds that are built of low-Z elements using laboratory X-ray radiation source.[31]

The density functional theory as well as the Møller–Plesset perturbation theory calculations for the isolated $(BH_3NH_2BH_2NH_2BH_3)^-$ anion in the gas phase (Fig. 6) indicate that the C_{2v} form is less stable than the C_1 form. The relative energy of the C_1 isomer with respect to the C_{2v} one (corrected for the energy of zero-point vibrations) is around -0.15 ± 0.01 eV. However, because the energy difference is not significantly large, it may be anticipated that the interactions of anions with cations as well as the differences of packing lead to the small preference of the C_{2v} quasi-alkane form in the solid state.[32] These calculations also show that the hydride anions of the terminal BH_3 groups are the most basic (*i.e.* more negatively charged) H atoms of the anion, which provides further confirmation of their capability to coordinate with metal cations. Note that the B–N bond lengths of the C_{2v} form are close to the experimentally determined value of 1.59(6) Å.

We investigated the thermal stability of alkali M(B3N2) phases under inert argon atmosphere (at −35 °C, at room temperature and on heating to 200 °C, Fig. 7) in comparison to those of respective amidoboranes. It was noticed that LiAB, NaAB and $NaLi(AB)_2$ are unstable at room temperature and spontaneously decompose releasing hydrogen contaminated with ammonia.[17,22,23] After several days of storing the sample of light alkali amidoboranes at RT they are contaminated with the traces of M(B3N2) phases (for PXD patterns see ESI†). Contamination of LiAB and NaAB samples by the traces of Li(B3N2) and Na(B3N2) may be observed in PXD patterns reported in our previous reports[17,33] and independently by other groups[10,26,34] (ESI†). Furthermore, the heating of light alkali amidoborane samples to *ca.* 50 °C results in an accelerated formation of respective M(B3N2) phases (which can be detected by PXD) accompanied by the evolution of ammonia (Fig. 8):

$$3M(NH_2BH_3) \rightarrow [M(NH_3)](BH_3NH_2BH_2NH_2BH_3) + 2[M] \quad (3)$$

$$[M(NH_3)](BH_3NH_2BH_2NH_2BH_3) \rightarrow M(BH_3NH_2BH_2NH_2BH_3) + NH_3\uparrow \quad (4)$$

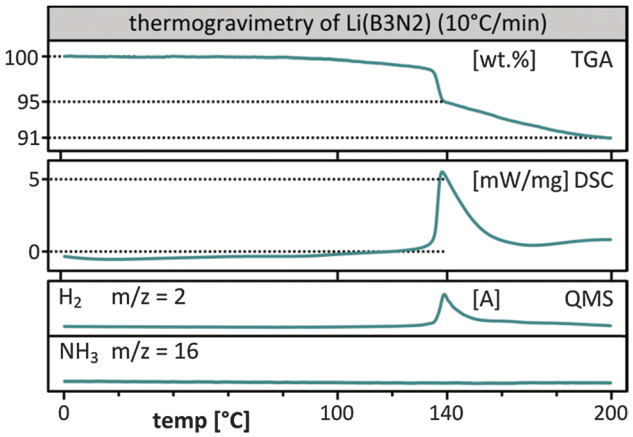

Fig. 7 The TGA/DSC profiles and well as the ion current for m/z = 2 (H_2) and 16 (NH_3) measured for the thermal decomposition of Li(B3N2) at 10 °C min^{-1} scanning rate.

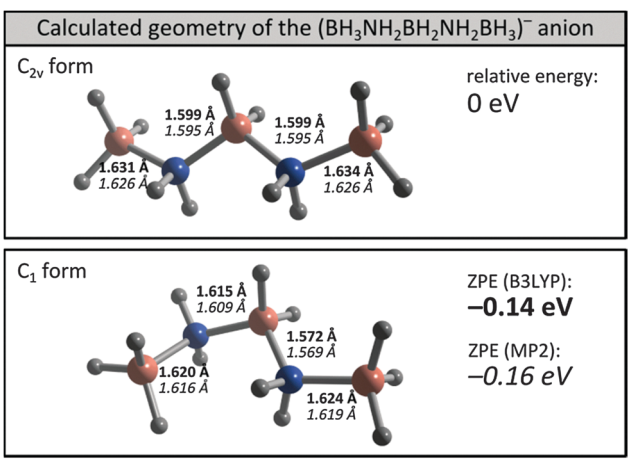

Fig. 6 The calculated geometry of the $(BH_3NH_2BH_2NH_2BH_3)^-$ anion in the C_{2v} form (top) and C_1 form (bottom) as optimized at the 6-311++G**/B3LYP (bold) or /MP2 (italics) level of theory. Zero-point vibrational energy-corrected relative energy is in eV.

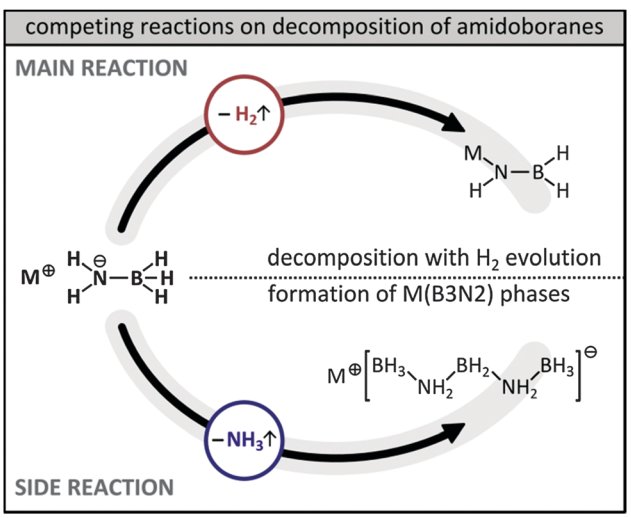

Fig. 8 The simplified mechanism of two competing reactions during the thermal decomposition of alkali metal amidoboranes: direct evolution of H_2 (top) and formation of M(B3N2) phases with the evolution of NH_3 (bottom).

where [M] in eqn (3) stands for unbalanced alkali metal, indicating that the true pathway for the decomposition reaction is more complex than the one proposed here. One possibility to balance eqn (3) is the formation of amorphous $M_2(NHBH_3)$ phases:

$$5M(NH_2BH_3) \rightarrow [M(NH_3)](BH_3NH_2BH_2NH_2BH_3) + 2M_2(NHBH_3) + H_2\uparrow \quad (5)$$

However, we choose not to speculate further about the mechanism of the side reaction due to the largely amorphous nature of the products as well as insufficient amount of experimental data.

Li(B3N2) and Na(B3N2) salts are considerably more thermally stable than their amidoborane analogues; they decompose exothermally at temperatures over 140–160 °C (Fig. 7 and ESI†).[25] Crystalline $LiBH_4$ and $NaBH_4$ were identified in the solid residues after the dehydrogenation of the respective M(B3N2) phases, suggesting the following tentative mechanism for the thermal decomposition:[17]

$$M(BH_3NH_2BH_2NH_2BH_3) \rightarrow MBH_4 + 2/n\ (NHBH)_n + 2H_2\uparrow \quad (6)$$

The expected mass loss according to eqn (6) is 5.0% (for Li salt). The first sudden mass loss observed for the Li sample at 140 °C is *ca.* 5 wt%, which is in a crude agreement with the simplified mechanism described by eqn (6). Additional mass loss is observed for temperatures up to 200 °C, which suggests that the resulting $(NHBH)_n$ also decomposes to some extent releasing H_2:

$$1/n\ (NHBH)_n \rightarrow BN + H_2\uparrow \quad (7)$$

Importantly, Li(B3N2) releases very pure H_2 gas, which is free from ammonia or any other N–B–H impurities. This feature (together with the increased total H content) represents a major advantage of Li(B3N2) phases over the pristine LiAB, which yields hydrogen severely contaminated with ammonia.[22,34,35]

Conclusions

We have synthesized and characterized two novel protonic-hydridic compounds, the lithium and sodium M(B3N2) derivatives containing the $(BH_3NH_2BH_2NH_2BH_3)^-$ anions. These lightweight salts constitute novel H-rich materials of high gravimetric and volumetric hydrogen capacity (12.6–15.1 wt% H); they are stable at room temperature. Li salt releases pure H_2 gas upon heating in the 140–200 °C temperature range, which is of immense importance for practical applications. This-along with the increased total H content-represent a major advantage of Li(B3N2) phases over the pristine LiAB, which yields H_2 severely contaminated with ammonia.[22,34,35] Metal borohydrides constitute the only crystalline products of the thermal decomposition of the M(B3N2) salts.

The spontaneous formation of M(B3N2) phases in the samples of LiAB, NaAB and $NaLi(AB)_2$ at room temperature changes the N : B balance of the solids from 1 : 1 to $\frac{2}{3}$: 1, which is related to the evolution of ammonia impurity (along with H_2) from pristine MAB salts. The exact mechanism of formation of the M(B3N2) phases as a side reaction taking place during thermal decomposition of MAB phases is currently unknown. One of the assumed scenarios involve the short-lived intermediates containing related but shorter B2N backbone that are similar to NaB_2H_8N reported in the 1930s,[24] but more experimental evidence is needed to confirm it.

Experimental

Synthetic procedures

Alkali metal M(B3N2) phases and amidoboranes were synthesized by the direct reaction of alkali metal hydride with ammonia borane in dry THF under the argon gas atmosphere. Reagents of the highest commercially available purity have been used: LiH, $LiNH_2$, NaH (95%, Sigma Aldrich) and NH_3BH_3 (98%, JSC Aviabor). THF (99.9%, Sigma Aldrich) was firstly dried over yttrium borohydride or sodium hydride and then distilled.

Synthesis of M(B3N2) phases (eqn (8)) and amidoboranes (eqn (9) and (10)) were performed according to the following reaction equations:

$$MH + 3NH_3BH_3 \rightarrow M(BH_3NH_2BH_2NH_2BH_3) + NH_3\uparrow \quad (8)$$

$$MNH_2 + NH_3BH_3 \rightarrow MNH_2BH_3 + H_2\uparrow \quad (9)$$

$$MH + NH_3BH_3 \rightarrow MNH_2BH_3 + H_2\uparrow \quad (10)$$

Reactions were performed in THF solution at room temperature with continuous stirring for 24 h or in a disc mill by mechanosynthetic method. The solid products were washed several times with fresh portions of THF and allowed to dry; they were analyzed without further purification. Samples were stored under argon atmosphere in Labmaster DP MBRAUN glovebox ($O_2 < 1.0$ ppm; $H_2O < 1.0$ ppm) at −35 °C. All further analyses were performed under inert atmosphere or in vacuum.

Thermal decomposition was investigated using an STA 409 simultaneous thermal analyzer from Netzsch, in the temperature range of −10 °C to +350 °C. STA 409 allows for the simultaneous thermogravimetric analysis (TGA), differential scanning calorimetry (DSC) and evolved gas analysis (QMS). The samples were loaded into alumina crucibles. High purity 6 N argon was used as a carrier gas. The evolved gases were analyzed with a QMS 403C Aëolos mass spectrometer from Pfeiffer-Vacuum. Transfer line was preheated to 200 °C to avoid the condensation of residues.

Infrared absorption spectroscopy

All substrates, products and thermally decomposed samples were characterized with infrared absorption spectroscopy in KBr pellets using a Vertex 80v vacuum FTIR spectrometer from Bruker. The samples sealed in a 0.6 mm thick quartz capillary under Ar were also characterized by Raman spectroscopy using a custom designed setup for micro-Raman spectroscopy based on monochromator Jobin Yvon THR1000 with CCD detection. Excitation line 632.8 nm was used.

Powder X-ray diffraction

PXD patterns of solids (sealed under argon inside 0.6 mm thick quartz capillaries) were measured using two diffractometers: (a) Panalytical X'Pert Pro diffractometer with linear PIXcel Medipix2 detector (parallel beam; the $CoK_{\alpha 1}$ and $CoK_{\alpha 2}$ radiation intensity ratio of *ca.* 2 : 1, $\lambda \sim 1.789$ Å), denoted here as CoK_{α}; (b) Bruker D8 Discover diffractometer with 2D Vantec detector (parallel beam; the $CuK_{\alpha 1}$ and $CuK_{\alpha 2}$ radiation intensity ratio of *ca.* 2 : 1, $\lambda \sim 1.5406$ Å), denoted here as CuK_{α}. All the PXD results are shown in copper scale.

The diffraction signals of M(B3N2) phases, M = Li or Na, were indexed using X-cell program[36] (Accelrys). Because of the significant disorder and presence of peaks from unidentified impurities, the successful structure solution was only possible after the proper identification of the anions from spectroscopic methods (M = Li or Na) and information on the BNBNB backbone from the single crystal diffraction (M = Na). In both the cases, the structure solution was attempted in several unit cells using a real-space method implemented in program FOX.[37] Finally, because the unit cells of lower symmetry did not lead to the significant improvement of fit, we chose the high-symmetry solutions, which very efficiently reproduced the experimental patterns and refined the starting models in Jana2006.[38] Several restraints were necessary to retain the realistic geometry of the anions for M = Li or Na; all the N–H and B–H distances and angles related to hydrogen atoms were restrained to 1.10(1) Å, and 109.5(5)° (M = Li) or 109.47(5)° (M = Na), respectively; for M = Na B–N distances were also restrained to 1.60(1) Å; the atomic displacement parameters (ADP) of H atoms were set as 1.2–1.5 of ADP of adjacent heavier atom. The weak scattering of X-ray by hydrogen atoms allows for only rough determination of their positions, therefore all the distances involving hydrogen atoms should be treated as an approximate approach. The pseudo-Voigt peak shape function was used; the background has been manually modeled. Further details of the crystal structure investigation(s) may be obtained from the Fachinformationszentrum Karlsruhe, 76344 Eggenstein-Leopoldshafen (Germany), on quoting the depository CSD numbers: 428007 – $Li(B_3N_2H_{12})$, 428008 – $Na(B_3N_2H_{12})$.

^{11}B NMR spectra of M(B3N2) phases and respective amidoboranes were obtained using a NMR UnityPlus 200 MHz VARIAN spectrometer with $BF_3{:}C_2H_5{-}O{-}C_2H_5$ as an external standard and ^1H NMR measurements were performed with TMS. $THFd_8$ (Aldrich, 99.5 atom% D), dried over metallic sodium, was used as a solvent.

Acknowledgements

To Mr Jerzy Antoni Fijalkowski on his birthday. This research was funded from 0122/IP3/2011/71 grant ''Iuventus Plus'' of the Polish Ministry of Science and Higher Education. E.M.-P. and T.P. gratefully acknowledge the support of the Polish National Science Center (project no. 2011/01/M/ST3/00855) (program ''Harmonia''). The authors would like to thank Dr Armand Budzianowski for preliminary solving the crystal structure of NaAB (to be published elsewhere).

Notes and references

1 W. Grochala and P. P. Edwards, *Chem. Rev.*, 2004, **104**, 1283.
2 Ł. Maj and W. Grochala, *Adv. Funct. Mater.*, 2006, **16**, 2061.
3 C. W. Hamilton, R. T. Baker, A. Staubitzc and I. Manners, *Chem. Soc. Rev.*, 2009, **38**, 279.
4 A. J. Churchard, E. Banach, A. Borgschulte, R. Caputo, J.-C. Chen, D. Clary, K. J. Fijalkowski, H. Geerlings, R. V. Genova, W. Grochala, T. Jaron, J. C. Juanes-Marcos, B. Kasemo, G. J. Kroes, I. Ljubic, N. Naujok, J. K. Norskov, R. A. Olsen, F. Pendolino, A. Remhof, L. Romanszki, A. Tekin, T. Vegge, M. Zach and A. Zuttel, *Phys. Chem. Chem. Phys.*, 2011, **13**, 16955.
5 F. E. Pinkerton, G. Meisner, M. Meyer, M. Balogh and M. J. Kundrat, *J. Phys. Chem. B*, 2005, **109**, 6.
6 Z. Xiong, G. Wu, J. Hu and P. Chen, *Adv. Mater.*, 2004, **16**, 1522.
7 R. W. Parry, D. R. Schultz and P. R. Girardot, *J. Am. Chem. Soc.*, 1958, **80**, 1.
8 S. G. Shore and R. W. Parry, *J. Am. Chem. Soc.*, 1955, **77**, 6084–6085.
9 J. Baumann, E. Baitalow and G. Wolf, *Thermochim. Acta*, 2005, **430**, 9.
10 Z. Xiong, C. K. Yong, G. Wu, P. Chen, W. Shaw, A. Karkamkar, T. Autrey, M. O. Jones, S. R. Johnson, P. P. Edwards and W. I. F. David, *Nat. Mater.*, 2008, **7**, 138.
11 H. V. K. Diyabalanage, T. Nakagawa, R. P. Shrestha, T. A. Semelsberger, B. L. Davis, B. L. Scott, A. K. Burrell, W. I. F. David, K. R. Ryan, M. Owen Jones and P. P. Edwards, *J. Am. Chem. Soc.*, 2010, **132**, 11836.
12 J. Luo, X. Kang and P. Wang, *Energy Environ. Sci.*, 2012, **6**, 1018–1025.
13 H. V. K. Diyabalanage, R. P. Shrestha, T. A. Semelsberger, B. L. Scott, M. E. Bowden, B. L. Davis and A. K. Burrell, *Angew. Chem., Int. Ed.*, 2007, **46**, 8995.
14 J. Spielmann, G. Jansen, H. Bandmann and S. Harder, *Angew. Chem., Int. Ed.*, 2008, **47**, 6290.
15 Q. Zhang, Ch. Tang, Ch. Fang, F. Fang, D. Sun, L. Ouyang and M. Zhu, *J. Phys. Chem. C*, 2010, **114**, 1709.
16 R. V. Genova, K. J. Fijalkowski, A. Budzianowski and W. Grochala, *J. Alloys Compd.*, 2010, **499**, 144.
17 K. J. Fijalkowski, R. V. Genova, Y. Filinchuk, A. Budzianowski, M. Derzsi, T. Jaroń, P. Leszczyński and W. Grochala, *Dalton Trans.*, 2011, **40**, 4407.
18 Y. Zhang, K. Shimoda, T. Ichikawa and Y. Kojima, *J. Phys. Chem.*, 2010, **114**, 14662.
19 W. Li, L. Miao, R. H. Scheicher, Z. Xiong, G. Wu, C. M. Araujo, A. Blomqvist, R. Ahuja, Y. Feng and P. Chen, *Dalton Trans.*, 2012, **41**, 4754.
20 X. Kang, J. Luo, Q. Zhang and P. Wang, *Dalton Trans.*, 2011, **40**, 3799.

21 H. Wu, W. Zhou, F. E. Pinkerton, M. S. Meyer, Q. Yao, S. Gadipelli, T. J. Udovic, T. Yildirim and J. J. Rush, *Chem. Commun.*, 2011, **47**, 4102.
22 K. J. Fijalkowski and W. Grochala, *J. Mater. Chem.*, 2009, **19**, 2043.
23 K. J. Fijalkowski, R. Jurczakowski, W. Kozminski and W. Grochala, *Phys. Chem. Chem. Phys.*, 2012, **14**, 5778.
24 H. I. Schlesinger and A. B. Burg, *J. Am. Chem. Soc.*, 1938, **60**, 290.
25 I. C. Evans, PhD dissertation, University of Birmingham, 2011.
26 K. R. Ryan, PhD dissertation, University of Oxford, 2011.
27 W. C. Ewing, P. J. Carroll and L. G. Sneddon, *Inorg. Chem.*, 2013, **52**, 10690.
28 H. Wu, W. Zhou and T. Yildirim, *J. Am. Chem. Soc.*, 2008, **130**, 14834.
29 J.-Ph. Soulié, G. Renaudin, R. Černý and K. Yvon, *J. Alloys Compd.*, 2002, **346**, 200.
30 R. S. Kumar and A. L. Cornelius, *Appl. Phys. Lett.*, 2005, **87**, 261915.
31 Crystallographic density of both M(B3N2) salts is quite low, about 0.96 g cm^{-3} for M = Li and 1.09 g cm^{-3} for M = Na, but in the range typical for the H-rich salts of these metals.
32 The Rietveld fit of the crystal structure of Na(B3N2) is of somewhat poorer quality than that for its lithium analogue. It could be due to the presence of a fraction of the C_1-like anionic moieties in the crystal structure model, which improve fit parameters. We have not tried this due to a generally weak diffraction was obtained from this sample.
33 *E.g.*, in our paper, we have noticed an unknown impurity on $NaLi(AB)_2$, which was denoted as "*P*1 phase" (ref. 17) which has now been identified as Na(B3N2).
34 C. Wu, G. Wu, Z. Xiong, W. I. F. David, K. R. Ryan, M. O. Jones, P. P. Edwards, H. Chu and P. Chen, *Inorg. Chem.*, 2010, **49**, 4319.
35 *Cf.*: Y. S. Chua, P. Chen, G. Wu and Z. Xiong, *Chem. Commun.*, 2011, **47**, 5116, and references therein.
36 M. A. Neumann, *J. Appl. Crystallogr.*, 2003, **36**, 356.
37 V. Favre-Nicolin and R. Černý, *J. Appl. Crystallogr.*, 2002, **35**, 734.
38 V. Petricek, M. Dusek and L. Palatinus, *Jana2006. Structure Determination Software Programs*, Institute of Physics, Praha, Czech Republic, 2006.

